Video Article

Autoradiography As a Simple and Powerful Method for Visualization and Characterization of Pharmacological Targets

Nane Griem-Krey[1], Anders Bue Klein[1], Matthias Herth[1,2,3], Petrine Wellendorph[1]

[1]Department of Drug Design and Pharmacology, Faculty of Health and Medical Sciences, University of Copenhagen

[2]Neurobiology Research Unit and CIMBI, Copenhagen University Hospital

[3]Department of Clinical Physiology, Nuclear Medicine & PET, Copenhagen University Hospital

Correspondence to: Petrine Wellendorph at pw@sund.ku.dk

URL: https://www.jove.com/video/58879
DOI: doi:10.3791/58879

Keywords: Radioligand, radioactive, autoradiography, affinity, expression, phosphor imaging, HOCPCA, γ-hydroxybutyric acid, GHB, NCS-382, quantitative pharmacology

Date Published: 10/26/2018

Citation: Griem-Krey, N., Klein, A.B., Herth, M., Wellendorph, P. Autoradiography As a Simple and Powerful Method for Visualization and Characterization of Pharmacological Targets. *J. Vis. Exp.* (), e58879, doi:10.3791/58879 (2018).

Abstract

In vitro autoradiography aims to visualize the anatomical distribution of a protein of interest in tissue from experimental animals as well as humans. The method is based on the specific binding of a radioligand to its biological target. Therefore, frozen tissue sections are incubated with radioligand solution, and the binding to the target is subsequently localized by the detection of radioactive decay, for example, by using photosensitive film or phosphor imaging plates. Resulting digital autoradiograms display remarkable spatial resolution, which enables quantification and localization of radioligand binding in distinct anatomical structures. Moreover, quantification allows for the pharmacological characterization of ligand affinity by means of dissociation constants (K_d), inhibition constants (K_i) as well as the density of binding sites (B_{max}) in selected tissues. Thus, the method provides information about both target localization and ligand selectivity. Here, the technique is exemplified with autoradiographic characterization of the high-affinity γ-hydroxybutyric acid (GHB) binding sites in mammalian brain tissue, with special emphasis on methodological considerations regarding the binding assay parameters, the choice of the radioligand and the detection method.

Introduction

Autoradiography is a method which provides images of radioactive decay. The technique is routinely used to study the tissue distribution of a protein of interest *in vitro* based on a specific pharmacological interaction between a radiolabelled compound and its target. This provides direct information about the selectivity of the ligand for the target. *In vitro* autoradiography may also be used for quantitative determination of pharmacological binding parameters of radioligands, such as the dissociation constant (K_d) and density of binding sites (B_{max}), as well as for determining the inhibition constant (K_i) of competing ligands[1,2]. Compared to traditional homogenate radioligand binding, autoradiography has the advantage of being able to visualize spatial anatomy and giving succinct details of regional expression patterns[3]. The method of autoradiography is therefore a relevant alternative to immunocytochemistry, especially in the absence of a validated antibody. Autoradiography is easily implemented in a standard radioisotope laboratory given the availability of a suitable radioligand with the required pharmacological specificity, access to a microtome cryostat for preparing tissue sections, and a suitable imaging device that is able to analyze the distribution of radioactivity in the respective tissue sections. Notably, an important selection criterion for the radioligand is a limited amount of binding to non-target sites. This can be to other proteins, membranes or materials such as plastic or filters, and is collectively referred to as non-specific binding. Usually, non-specific binding is non-saturable but can be saturable if it involves a specific off-target protein. The best way of validating true specific binding is to compare to tissues lacking the target, *e.g.*, genetically engineered (knock-out) tissue[4].

Here, the methodology is illustrated with the autoradiographic characterization of the high-affinity binding site for γ-hydroxybutyric acid (GHB) in the mammalian brain. Understanding the pharmacological interaction between GHB and its binding site is of relevance as GHB is both a clinically useful drug in the treatment of narcolepsy and alcoholism[5], but also a natural constituent of the mammalian brain and a recreational drug[6]. High-affinity GHB binding sites were first described using [^{3}H]GHB binding to rat brain homogenate[7]. Over the years, further autoradiography studies with [^{3}H]GHB and the analogue [^{3}H]NCS-382 has showed a high density of binding sites in forebrain regions of rat[8,9,10], mouse[9], pig[11]and monkey/human brain[12]. However, the molecular identity and exact functional relevance of these binding sites have remained elusive.

With the intention to further characterize the binding sites, and to facilitate studies on the physiological role of GHB, multiple radioligands incorporating different isotopes endowed with different affinities have been developed ([^{3}H]GHB, [^{3}H]NCS-382, [^{3}H]HOCPCA and [^{125}I]BnOPh-GHB)[13,14,15,16](reviewed in[17]) (**Figure 1**). The combination of selective high-affinity radioligands and a very high tissue density of the binding sites have allowed for the production of high-quality images using the phosphor imaging technique[9,11]. Along with an outline of the practical points in setting up an autoradiographic experiment and an illustration to exemplify details, the discussion section will emphasize i) the choice of radionuclide, ii) the choice of assay conditions, and iii) the use of phosphor imaging plates versus X-ray film. The overall goal of this paper is to provide technical, methodological and scientific details on the autoradiography technique for informing about tissue distribution and pharmacological analysis of protein targets.

Protocol

All animal handling was performed in compliance with the guidelines from The Danish Animal Experimentation Inspectorate.

NOTE: The protocol described here covers tissue preparation (*i.e.*, mouse brain tissue), the *in vitro* autoradiographic assay in sufficient detail for setting up the method in a new lab, the exposure to phosphor imaging plates as well as subsequent densitometric analysis of autoradiograms (**Figure 2**) with the aim of localizing and quantifying radioligand binding in distinct anatomical structures. For histological comparison, a protocol for cresyl violet staining is included. Moreover, the determination of non-specific binding with a competing ligand is included within the protocol. For a detailed description on how to determine K_d, B_{max} or K_i, see previous publication[4].

1. Tissue Preparation by Cryosectioning

1. Euthanize the mouse by cervical dislocation and immediately dissect out the brain using scissors and forceps. Directly proceed to the next step to avoid tissue damage.
2. Snap-freeze the tissue by submersion in powdered dry ice, gaseous CO_2 or isopentane. Directly transfer the frozen tissue to a cryostat with the temperature set to -20 °C. Alternatively, store the tissue at -80 °C until processing.
   NOTE: Avoid repeated thawing/freezing to reduce tissue damage.
3. Let the tissue acclimate to -20 °C in the cryostat for 20 min before further processing to avoid tissue shattering.
4. Cover the tissue holder with embedding medium outside the cryostat and quickly place the frozen tissue specimen in the desired orientation while the embedding medium is still liquid. For instance, place the mouse brain vertically onto cerebellum in order to achieve rostral coronal sections. Transfer the tissue holder back to the cryostat and expose the embedding medium to temperatures below -10 °C for hardening.
   NOTE: Fragile tissue specimen should be coated in embedding medium within the tissue molds prior to mounting.
5. Position the tissue holder in the microtome of the cryostat. Adjust the orientation of the tissue to avoid sloped sections.
6. Cut the tissue with the guidance of a stereotaxic atlas[18] in sections of desired thickness (12 µm recommended for [^{3}H] labelled ligands). Carefully straighten and unfold the section with a brush of small size if necessary and thaw-mount the section onto a microscope slide. Sequentially collect the sections from the region of interest for desired technical replication (*e.g.*, 4 sections per slide).
7. Allow the sections on the slides to air-dry for 1 h before further handling.
   NOTE: Addition of desiccant material to slide boxes minimizes moisture build up on the tissue sections. Procotol can be paused here by storing sections long-term in slide boxes at -80 °C.

2. *In vitro* Autoradiography

CAUTION: Radioactivity. Work in a certified laboratory according to local regulations. Wear protective clothing. Dispose in accordance with radioactive decay or outsource to a certified company.

1. Thaw the sections for at least 30 min at room temperature (RT). Label the slides with experimental conditions. Use a pencil because the slides will be bathed in ethanol during subsequent staining.
2. Place the slides horizontally in plastic trays.
   NOTE: Positioning slides on an elevated platform within plastic trays facilitates their handling.
3. Pre-incubate the sections mounted on the slides in assay buffer adjusted to target in question (for GHB protocol, 50 mM $KHPO_4$ buffer pH 6.0 is used) by carefully applying an appropriate volume onto the slide (700 µL for 3-4 rodent coronal sections).
   NOTE: Make sure that every section is covered completely with liquid.
   1. Cover the plastic trays with a lid in order to avoid evaporation and pre-incubate at relevant temperature (for GHB protocol pre-incubate for 30 min at RT) under constant gentle (20 rpm) shaking on a plate shaker.
   2. For the determination of non-specific binding, supplement assay buffer with relevant concentration of unlabelled compound (for GHB protocol, 1 mM GHB).
      NOTE: Pre-incubation may not be necessary.
4. Pour off pre-incubation liquid from each slide and transfer the slides back to the plastic tray.
5. To avoid dehydration, immediately incubate the sections with relevant concentration of radioligand in assay buffer under desired conditions (for GHB protocol, 1 nM [^{3}H]HOCPCA for 1 h at RT) by covering the sections completely with the radioligand solution (700 µL for 3-4 rodent coronal sections).
   1. Incubate under under constant gentle (20 rpm) shaking of plastic trays with closed lid.
      NOTE: The radioligand concentration can be validated by counting an aliquot in a liquid scintillation counter.
6. Remove the incubation solution by pouring off the liquid and transfer the slides into a microscope slide rack. Immediately proceed to the next step to avoid section dehydration.
7. Wash the slides. For the GHB protocol, wash with ice-cold assay buffer twice for 20 s and then rinse twice by dipping the slide rack into the trays filled with ice-cold distilled water to remove salts. Position the slides vertically in racks for air-drying for at least 1 h at RT or dry the slides for 5 min with a blower set to cold temperature.
   NOTE: Washing must be optimized, *e.g.*, extensive washing may be useful for decreasing non-specific binding.
8. Transfer the slides to a fixator containing paraformaldehyde (PFA) powder for overnight fixation with PFA vapours at RT in order to protect the integrity of the ligand-target complex.
   CAUTION: PFA is toxic. Positionthe fixator in fume hood and avoid skin/eye contact with PFA.
9. The following day, transfer the slides to a desiccator box containing silica gel for 3 h at RT to eliminate moisture.

3. Exposure to Phosphor Imaging Plates and Scanning

1. Place the sections in a radiation-shielded imaging plate cassette with the tissue facing up. For subsequent quantification of radioligand binding, include a [^{3}H]microscale in every cassette. Arrange the sections randomly and expose the sections for direct comparison in the same cassette.
2. Erase the tritium-sensitive phosphor imaging plate immediately before usage in order to remove accumulated signals from storage and to eliminate background signals. Therefore, load the plate into phosphor imaging machine and expose it to visible/infrared light according to the instructions of the manufacturer.
3. Remove the plate from phosphor imaging machine and immediately place it onto the sections in the cassette. Make sure that the cassette is closed completely. Expose the sections to the phosphor imaging plate for 3 days at RT shielded from light.
4. Because light erases signal from the imaging plate, carefully open the cassette in the dark and immediately transfer the imaging plate into the dark box of a phosphor imager or place the phosphor imager in a dark room.
   NOTE: Make sure to notate the spatial arrangement of the slides during exposure in order to identify individual specimen on the digital image after analysis. Therefore, phosphor imaging plates also display one corner cut in a distinct angle in order to identify the correct orientation of the plate on the digital picture.
5. Scan the plate at the highest resolution possible to obtain a digital image.

4. Optional: Cresyl Violet Staining of Tissue Sections

1. Prepare 1% cresyl violet solution by mixing 5 g of cresyl violet acetate in 500 mL of deionized water (dH_2O) until dissolved (approximately 2 h). Filter through a filter paper using a funnel into a new 500 mL bottle. Adjust pH to 3.5-3.8.
2. Position the slide staining set under fume hood. Prepare trays with the following solutions in white polypropylene trays (except for xylene):
   a. 50% ethanol/50% dH_2O
   b. 70% ethanol/30% dH_2O
   c. 100% ethanol
   d. 100% ethanol
   e. 100% dH_2O
   f. 1% cresyl violet
   g. 0.07% acetic acid (add 175 µL of acetic acid to 250 mL of dH_2O).
   h. 100% xylene in green solvent-resistant trays
   i. 100% xylene in green solvent-resistant trays
3. Transfer the slides to the fume hood and place them in a slide rack.
4. Dissolve the lipids through increasing graded series of ethanol in dH_2O into 100% ethanol (tray a-d) by dipping the slides for 1 min.
5. Rehydrate the specimens to dH_2O through descending concentrations of ethanol (tray a-d in reverse order, followed by tray e) by dipping the slides for 1 min.
6. Immerse the specimens in cresyl violet solution for 10 min.
7. Rinse the specimens in 0.07% acetic acid by lifting the slides up and down gently for 4-8 s. Wash the slides by dipping in dH_2O for 1 min.
8. Dehydrate the specimens by immersion of the slides for 30 s in ascending concentrations of ethanol (tray a-d).
9. Transfer the specimens through two trays of 100% xylene (tray h and i) to quench the ethanol.
10. Rehydrate the specimens to dH_2O through descending concentrations of ethanol (tray a-d in reverse order, followed by tray e) by dipping the slides for 1 min.
11. Remove the slides from saline with forceps. Add a few drops of organic solvent mounting media per slide and add a 24 x 60 mm coverslip on top to protect specimens. Remove air bubbles between the specimen and coverslip by gently pressing onto the coverslip.
    NOTE: Keep the remaining slides in xylene during mounting to prevent drying.
12. Dry the slides overnight in a fume hood at RT.
13. Obtain a picture of specimen with a microscope and 1.25X objective.

5. Densitometric Analysis of Digital Image

1. Measure relative optical densities (RODs) of each calibration standard from the [^{3}H]microscale with an image analysis software.
   1. Select an area of equal size for each point of the [^{3}H]microscale using a tool for **Region creation** from the menu item **Region determination**. Assign a number to each selected area by clicking on **Number** under the menu item **Label**.
   2. Export OD values for each point of the calibration standard by clicking **File | Export | 2D region report**. Transfer ROD values to a spreadsheet and normalize by the size of the selected area. Perform linear regression to obtain a standard curve for further densitometric analysis.
      NOTE: Make sure that the selected areas are labelled in order to identify matching ROD values and samples.

2. Perform quantification of autoradiograms using the proprietary imaging software by selecting the region of interest (ROI) using a **Region creation** tool in every section and measuring its ODs. Select the same region in every section by creating a template for the region of interest, which is copied and manually adjusted to minor variations in brain anatomy for each autoradiogram. Identify the anatomy of the ROI by comparison of autoradiograms with a brain atlas[18]. When multiple treatments are compared, perform the analysis blinded and randomized in order to avoid biased selection of ROIs.
3. Export ROD values and sizes of selected areas into a spreadsheet by clicking **File | Export | 2D region report**.
4. Divide the measured ROD of the selected ROI by its area to obtain the density per specific area.
5. Measure the ROD of the background of the plate and export corresponding ROD values and area size into a spreadsheet. Subtract the average background signal from every ROD value of each ROI.
6. Average the RODs of technical replicates, *i.e.*, section replicates using tissue from the same animal.
7. Use the standard curve to convert RODs into units of radioligand binding, *i.e.*, nCi/mg tissue equivalents (TE).

NOTE: The term TE is used because standards are generated with materials simulating tissue.

8. Express binding by conversion of nCi/mg to fmol/mg TE according to the specific activity of the radioligand (Equation 1).

$$\text{ligand binding}\left[\frac{\text{fmol}}{\text{mg}}\ \text{TE}\right] = 1000 * \frac{\text{binding}\left[\frac{\text{nCi}}{\text{mg}}\ \text{TE}\right]}{\text{specific activity}\left[\frac{\text{Ci}}{\text{mmol}}\right]} \quad (1)$$

9. To obtain specific binding values, subtract non-specific binding from total binding.
10. Average the binding of every biological replicate by using the average of the technical replicates of each animal (obtained in Step 5.6).

Representative Results

Using the described protocol, the anatomical distribution of the high-affinity GHB binding sites was visualized with the radiolabelled GHB analogue [^{3}H]HOCPCA in mouse brain, which was cut into coronal, sagittal and horizontal sections (**Figure 3**). High levels of binding were observed in hippocampus and cortex, lower binding in striatum and no binding was detected in cerebellum, corresponding to previous reported expression patterns of the high-affinity GHB sites[9,10,11,12]. As shown here, the anatomical structures may be visualized using different sectioning planes and anatomical integrity may be supported by cresyl violet staining. For GHB high-affinity binding sites, especially regions with low radioligand binding, such as cerebellum, are confirmed with subsequent staining of the tissue (**Figure 3**). Coronal sections are most often found in the literature[9,10]. They are practical for quantitative purposes as a higher amount of sections can be obtained from one brain. Sagittal and horizontal sections have the advantage of visualizing binding throughout most of the rodent brain within one section thus providing great overview. **Figure 4**illustrates the evolutionary conservation of the high-affinity GHB binding sites in the mammalian brain. [^{3}H]HOCPCA binding sites were detected in mouse, rat as well as in pig brain tissue enabling comparison of gross brain anatomy between species. Generally, evolutionary conservation and regional distribution studies may aid significantly in the characterization of a protein of interest, in this case a novel target, and may thus give indications about its physiological function[19].

The high-affinity GHB binding sites were probed with GHB radioligands, which display different affinities for the binding sites but comparable specific activities (**Figure 5**). [^{3}H]HOCPCA was previously shown to have a K_d of 74 nM, which is superior to the commercially available radioligand [^{3}H]NCS-382 with a K_d of 697 nM, both determined at pH 6.0 by quantitative autoradiography[9]. Thus, [^{3}H]HOCPCA is endowed with much higher sensitivity, leading to an excellent signal-to-noise ratio. Due to the lower sensitivity of [^{3}H]NCS-382, higher radioligand concentrations must be used in order to obtain similar levels of binding (compare y-axes in **Figure 5**). When compared to [^{3}H]GHB, even higher radioligand concentrations (30 nM) are necessary to achieve comparable binding levels. This is predominantly due to the significantly lower affinity (K_i of 4.5 µM) of this radioligand[20]. However, higher radioligand concentration also increases the level of non-specific binding[9,10] with a consequently lower signal-to-noise ratio. This series of experiments highlights the importance of having a high-affinity radioligand for producing high-quality images.

Because the high-affinity GHB sites are expressed to so high levels in forebrain regions (60 pmol/mg[17]), the determination of pharmacological parameters by saturation curves is inherently difficult using standard tritium sensitive phosphor imaging plates due to the risk of oversaturated images. Therefore, K_d values for [^{3}H]HOCPCA and [^{3}H]NCS-382 have been obtained by first determining K_i values by homologous displacement curves, and then calculation of K_d (**Figure 6**)[9]. For most radioligands, an alternative would be to use isotope-dilution as is routinely done in homogenate binding assays. Moreover, K_d values have been determined at different pH values. Evidently, the high-affinity GHB sites are most efficiently labelled at pH 6.0 (**Figure 6A** and **Figure 6D**), since changing assay conditions to pH 7.4 substantially impact ligand affinity. Thus, the K_d for [^{3}H]HOCPCA at pH 7.4 is approx. 30 times higher numerically than that at pH 6.0. Increasing the pH further results in a higher degree of non-specific binding, which becomes a caveat when using [^{3}H]NCS-382 where only low amounts of specific binding can be obtained at pH 7.4 (**Figure 6E**). This in fact hinders the determination of pharmacological parameters using this radioligand at physiological pH[9], again illustrating the power in having a radioligand with as high affinity as possible.

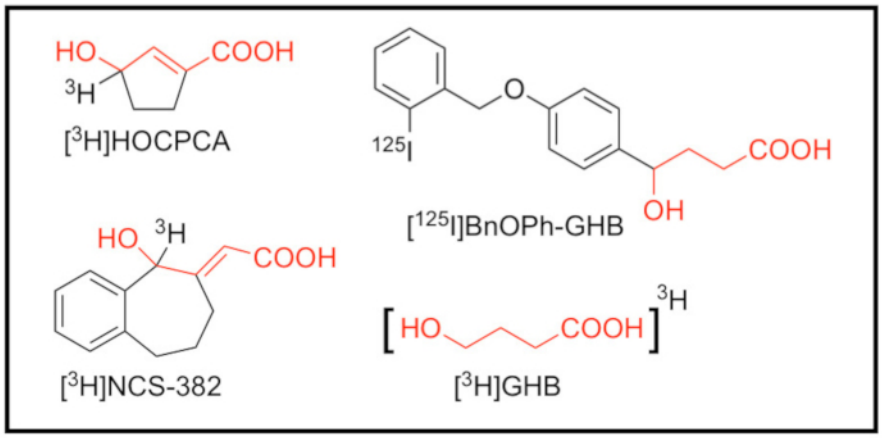

Figure 1: Structures of radioligands targeting the high-affinity GHB binding sites. [^{3}H]3-hydroxycyclopent-1-ene carboxylic acid ([^{3}H]HOCPCA)[14], [^{3}H](*E,RS*)-6,7,8,9-tetrahydro-5-hydroxy-5*H*-benzocyclohept-6-ylidene acetic acid (NCS-382) ([^{3}H]NCS-382)[15] and [^{3}H]γ-hydroxybutyric acid ([^{3}H]GHB)[16] as tritiated radioligands with comparable specific activity (20-40 Ci/mmol), as well as [^{125}I]4-hydroxy-4-[4-(2-iodoben-zyloxy)phenyl]butanoate ([^{125}I]BnOPh-GHB)[13] with an estimated molar activity of 2000 Ci/mmol[21]. The GHB structural element is highlighted in red. Please click here to view a larger version of this figure.

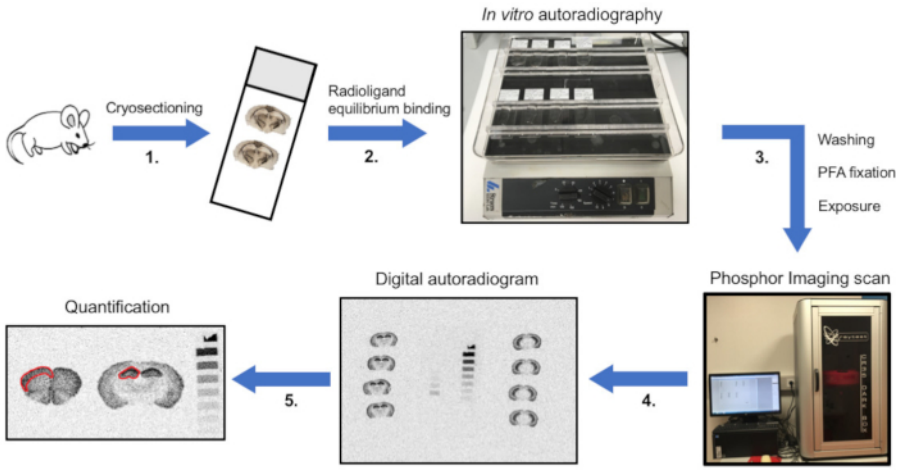

Figure 2: Schematic overview of the protocol of *in vitro* autoradiography. (1) The animal is euthanized, tissue is dissected and snap-frozen on dry ice. Tissue is then sectioned on a cryostat, thaw-mounted onto microscope slides and (2) sections are incubated with radioligand until equilibrium binding. For determination of non-specific binding, solutions are supplemented with an unlabelled displacer of a related but not identical chemical structure. (3) Subsequently, unbound radioligand is removed by washing in assay buffer and salts are eliminated by rinsing with distilled H_2O. When sections are dry, paraformaldehyde (PFA) fixation is performed to permanently establish the ligand-protein interaction. Sections are then exposed to phosphor imaging plates. (4) After sufficient exposure time, plates are scanned to obtain digital autoradiograms. (5) Ultimately, image analysis is performed using definitions of regions of interest (ROIs), and the binding is quantified. In the shown example, optical densities (ODs) are illustrated in sections of mouse cortex (left) and hippocampus (middle). Quantification is done by exposing sections together with a [^{3}H]microscale (right). Please click here to view a larger version of this figure.

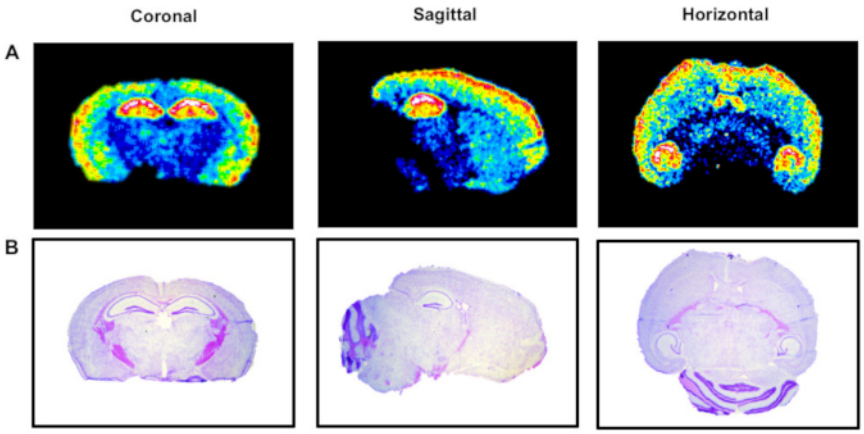

Figure 3: Representative autoradiograms of 1 nM [^{3}H]HOCPCA binding to mouse brain sections. (**A**) Radioligand binding to coronal, sagittal and horizontal tissue sections to illustrate the importance of the sectioning plane on the visibility of anatomical structures. (**B**) Cresyl violet staining of corresponding tissue sections to verify anatomical regions, particularly regions with low/absent radioligand binding. Please click here to view a larger version of this figure.

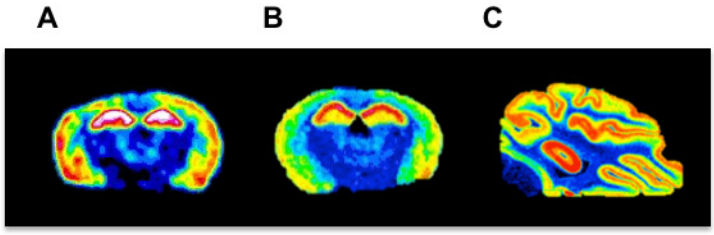

Figure 4: Representative autoradiograms of 1 nM [^{3}H]HOCPCA binding in different species. Comparison of (**A**) rat, (**B**) mouse and (**C**) pig *in vitro* autoradiograms in order to illustrate evolutionary conservation of binding sites to cortical and hippocampal regions along with gross brain anatomy. Please click here to view a larger version of this figure.

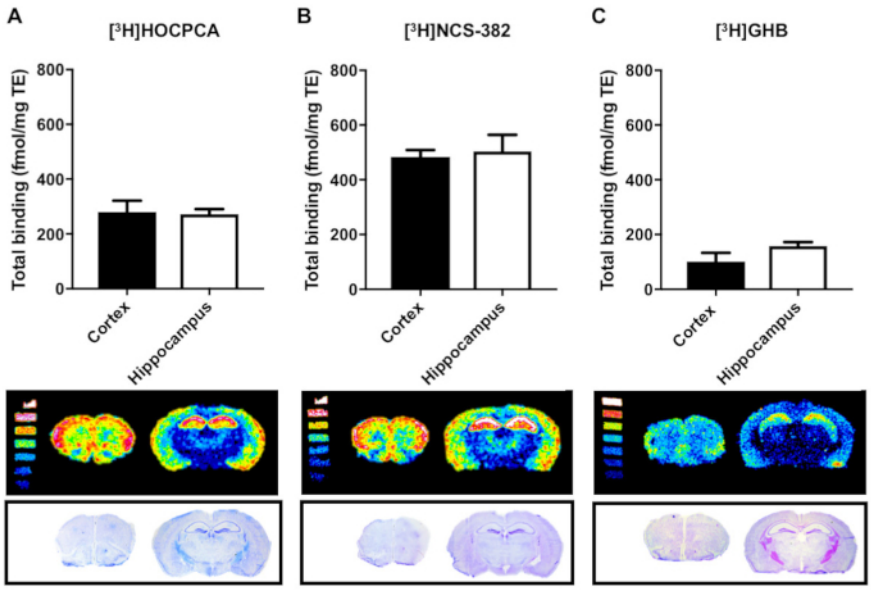

Figure 5: Quantification of binding to the high-affinity GHB binding sites with different sensitivity to GHB radioligands by *in vitro* autoradiography in brain slices from mouse cortex and hippocampus. Total binding is reported as fmol/mg tissue equivalents (TE) for the radioligands (**A**) [^{3}H]HOCPCA (1 nM) and (**B**) [^{3}H]NCS-382 (7 nM) and (**C**) [^{3}H]GHB (30 nM) (similar specific activities). Non-specific binding was not detected in the presence of 1 mM GHB or 1 mM HOCPCA for any of the radioligands (not shown). Data is presented as mean ± SD of four biological replicates each performed in three technical replicates. Please click here to view a larger version of this figure.

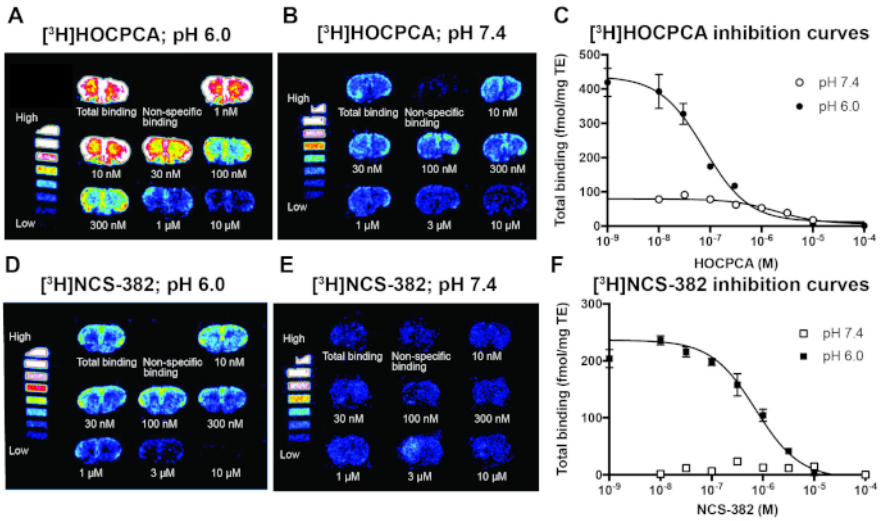

Figure 6: Representative results of autoradiographic determination of K_d and B_{max} values by homologous competitive displacement of [^{3}H]HOCPCA and [^{3}H]NCS-382 in mouse cortical sections at pH 6.0 and pH 7.4 in order to illustrate the influence of pH on affinity of radioligands. (K_d and B_{max} were calculated using the same compound as radioligand and competitor, through initial determination of K_i values[22]). (**A**) Autoradiograms with optimal signal-to-noise ratio for 1 nM [^{3}H]HOCPCA binding at pH 6.0. (**B**) Changing buffer pH to 7.4 requires a higher [^{3}H]HOCPCA concentration (8 nM) to reach significant binding levels. (**C**) Resulting log-concentration binding curves; mean ± SEM. (**D**) 5 nM [^{3}H]NCS-382 binding at pH 6.0 results in low non-specific binding, whereas (**E**) 40 nM [^{3}H]NCS-382 is insufficient to obtain binding at pH 7.4. (**F**) Resulting log-concentration binding curves; mean ± SEM. Data was obtained from 3-4 biological replicates each performed in 3-5 technical replicates, only [^{3}H]NCS-382 experiments at pH 7.4 were performed with only 2 biological replicates. For both radioligands, 1 mM GHB was used for the determination of non-specific binding. For details on analysis and calculation of K_d and B_{max}, see[9]. This figure has been adapted and reprinted from previous publication[9] with permission from Elsevier. Please click here to view a larger version of this figure.

Discussion

The quality of an autoradiographic assay is most often determined by the sensitivity of the radioligand. A major contributing factor is the selected radioisotope, which is given by the availability of known ligands or by the feasibility of specific labelling techniques to yield ligands with appropriate specific activity (*i.e.*, the amount of radioactivity per unit mole of a radioligand)[23]and with limited amounts of chemical degradation. A large number of radioligands of known ligands are labelled with tritium[9,10,24,25,26], which infers several advantages. Firstly, tritium (^{3}H) is characterized by a long half-life (12.43 years) promoting long-term storage of individual batches. Secondly, the ligand-target interaction is not distorted by the radionuclide as ^{3}H-ligands are biologically indistinguishable from their parent compounds. Tritium emits low energy β^--particles, which travel only short distances in tissue resulting in high spatial resolution and, subsequently, greater distinction between anatomical structures[4]. Nonetheless, tritium labelling can only be produced to yield moderately high specific activities. This is due to the fact that available ^{3}H-sources are contaminated with non-radioactive hydrogen. Generally, the higher the specific activity, the less radioligand is needed to yield sensitive detection[23]. Moreover, it should be considered that ^{3}H-ligands have the possibility to undergo hydrogen exchange with water depending on the stability of the ^{3}H-label. To compensate for low expression or too low specific activity, iodine-125 can be used as the radionuclide[13]. The maximal specific activity of iodine-125 is approx. 100-fold higher than that of tritium. However, several additional considerations have to be made when working with iodine-125. For instance, the addition of iodine-125 normally induces structural alterations in the molecule which may impact the ligand-target interactions. As iodine-125 has a half-life of 60 days, correction for daily decay should be considered for specific activity and quantification of ligand-target interactions[23]. ^{125}I-ligands emit γ-photons and in spite of much higher sensitivity, produce lower-resolution images. This is due to the inverse relationship between resolution and the maximum energy of the isotope (as discussed below). Finally, compared to tritium, increased care should be taken when handling iodine-125 due to the higher energy of the radionuclide.

Depending on the nuclide, tissue section thickness may influence resolution. The low-energy β^--radiation of tritium limits its tissue reach to approx. 5 µm due to self-absorption. As a consequence, quantification is not influenced by tissue thickness when the section thickness exceeds 5 µm[27,28]. By contrast, radioactive decay of high-energy isotopes has a greater tissue penetration, resulting in lower image resolution because ligands with a greater distance to the detection medium also contribute to image formation. Consequently, thinner sections promote higher resolution for high-energy radionuclides[1].

The establishment of an autoradiographic protocol requires knowledge of optimal binding conditions (*e.g.*, buffer, pH and temperature) and pharmacological parameters of the radioligand in terms of affinity and kinetics. If the radioligand has not been characterized before, exploratory studies are necessary[29]. Choosing an optimal radioligand concentration is guided both by the affinity of the radioligand and the abundance of binding sites. Normally, a concentration reflecting 5-6 times K_d is used to make sure that all binding sites are saturated[30]. Another approach aims to yield the highest ratio of total-to-non-specific binding by selecting radioligand concentrations below K_d[31] and saving radioligand solution at the same time. This approach is particularly useful when the binding site is highly abundant in the examined tissue since high radioligand concentrations would increase the chance of oversaturating autoradiograms, as the case for [^{3}H]HOCPCA and the high-affinity GHB binding sites[9]. Furthermore, in order to efficiently label the whole population of the targeted protein, the radioligand should ideally bind to all possible target conformations. Especially in receptor autoradiography, the use of agonists may only reveal a partial number of total receptors since some might be present in low-affinity agonist states. In contrast, neutral antagonists most often display affinity for all receptor states[26,29].

Moreover, binding experiments are generally performed under equilibrium binding conditions. Therefore, the time needed to reach equilibrium binding under the desired experimental conditions (fixed radioligand concentration, buffer and temperature) should be determined in association experiments to ensure equilibrium binding within the scope of the experiment[4,23,30]. After radioligand incubation, unbound radioligand is washed off by several incubations with assay buffer and typically followed by rinsing in distilled H_2O. Signal-to-noise ratios can be optimized by adjusting temperature and time depending on the dissociation rate of the radioligand[26,30,31].

Radioligands may display binding to non-biological materials, *i.e.*, non-specific binding. Radioligand binding to cellular components other than the intended target is defined as unspecific binding. The contribution of unspecific binding to the total amount of radioligand binding is assessed in the presence of a competing unlabelled ligand that targets the same binding site as the radioligand. As the non-radioactive compound (displacer) is supplied in 10,000-fold excess, it occupies the binding site and the radioligand can only bind to off-target sites[26,31,32]. Crucially, the unlabelled compound should be of a different chemical structure than the radioligand since this lowers the risk of displacing both specific as well as non-specific binding[23]. Non-specific binding arising from binding to membranes can be a major problem especially in the case of fairly lipophilic radioligands. In some cases, extensive washing procedures may remove non-receptor bound radioligand and therefore improve the specific binding ratios[29].

When choosing an assay buffer, it is crucial to consider the effect of ionic strength and pH on the ligand-target interaction. Especially electrostatic interactions between polar ligands and hydrophilic components of binding sites are influenced by the ionic strength of the buffer. Therefore, supplementation with monovalent or divalent ions may impact the effective affinity constant[23,33]. If the optimal buffer composition for the studied ligand-target interaction is unknown, different common buffers should be explored in pilot experiments. Buffers may also be supplemented with anti-oxidants such as ascorbic acid and inhibitors of degrading enzymes[29,34]. Moreover, the ionization of specific groups within the binding site or on the ligand itself is influenced by pH and has critical effects on the equilibrium binding constant, the kinetic rate constants and non-specific binding[23,33]. For example, probing the high-affinity GHB binding site with different GHB radioligands nicely illustrates the importance of pH on this binding target (**Figure 6**). Characterizing the optimal pH for the ligand-receptor interaction may also give clues about the importance of the target in relation to its biological relevance.

Another critical factor in digital autoradiography is the exposure time, *i.e.*, the time needed to achieve quantifiable autoradiograms by exposing the radiolabelled tissue sections to phosphor imaging plates. Estimates are based on the amount of radioactivity in the sample, the energy and half-life of the isotope as well as the desired signal-to-noise ratio. In particular, prolonged exposure time results in saturated images and high background signal. Elevated background signal can be reduced by storing cassettes within lead-shielded environments to avoid cosmic radiation[1,4]. Nevertheless, if suboptimal autoradiograms are achieved, the specimen can be exposed multiple times, provided that the ligand-target complex is fixed and the half-life of the radionuclide allows it.

Phosphor imaging plates can be reused and have a long lifespan when handled correctly, *i.e.*, bending should be avoided and plates should be stored in a dry environment. The handling of phosphor imaging plates is guided by their sensitivity to light and cosmic radiation. Thus, it is important to erase the plate prior to every use in order to minimize background signal. Exposure of radiolabelled tissue sections to the imaging plates is done in radiation-shielded cassettes completely devoid of light. When transferring the plate to the scanner at the end of the exposure time, any ambient light should also be avoided as even short contact with white light reduces accumulated signal. Furthermore, plates should be scanned immediately after the removal of the specimen to avoid signal fading. A drawback of using phosphor imaging plates is the potential appearance of artefacts and residual 'ghost images' after repeated usage of the plates[1].

Working with tritium requires imaging plates without a protective coating to allow the low energy radiation to reach the phosphor crystals. Tritium-sensitive phosphor imaging plates are therefore more sensitive to contamination or damage due to incorrect handling. Once contaminated, tritium-sensitive plates cannot be cleaned and need to be replaced. Fixation of the ligand-target complex with PFA vapour reduces potential contamination of the plate, lengthening its lifespan. Moreover, dehydration of the tissue subsequent to fixation is a crucial step since tritium sensitive plates are sensitive to moisture. Due to its delicate nature, tritium-sensitive plates should not be used for other isotopes[1,4]. In contrast, the plates for high-energy isotopes such as iodine-125 are more robust and their surface can even be cleaned by wiping with 70% ethanol.

Traditionally, radiosensitive film has been used for the spatial recording of radioactive decay. While images with high resolution can be obtained, film autoradiography has several limitations. Besides the necessity of hazardous chemicals and a darkroom for development, X-ray film is characterized by a narrow dynamic range. Therefore, it may be necessary to expose radiolabelled sections repeatedly with different exposure times in order to achieve quantifiable non-saturated images[35]. Moreover, X-ray film exhibits limited sensitivity resulting in sustained exposure times for specimen labelled with low energy isotopes, *i.e.* tritium decay may require several months of exposure. Low sensitivity combined with small linear range makes the technique extremely time consuming, especially when optimal assay conditions have to be determined first[1,35].

With the development of phosphor imaging plates, several of these limitations have been addressed[35,36,37]. The imaging plates serve to temporarily store images of radioactive decay, representing the spatial arrangement of radioligand in the tissue specimen. Photostimulable $BaFBr:Eu^{2+}$ phosphor crystals are used to capture the radioactive energy emitted by the sample, as high energy radiation (*e.g.,* X-rays, gamma rays or beta particles) results in the excitation of Eu^{2+} to Eu^{3+} and consequent trapping of the released electron in the phosphor lattice[4,37]. Exposing the imaging plate to visible or infrared light reverses the reaction, *i.e.,* the trapped electron is released and during the transformation of Eu^{3+} to Eu^{2+} luminescence is emitted. The emitted light is proportional to the amount of radioactivity and its detection by a photomultiplier enables the creation of a digital autoradiogram[37]. This system provides an increase in sensitivity accompanied by a marked reduction in exposure time from month to days[3]. On top of that, the linear dynamic range is considerably increased, which reduces the chance of oversaturated images. Linearity is given within four to five orders of magnitude and has been validated repeatedly[3,35,36,37,38]. Although film autoradiography still provides superior spatial resolution, efforts in scanning technology resulted in the improvement of resolution from 300 to 25 µm (pixel size), allowing the detailed differentiation between anatomical regions[3]. Overall, phosphor imaging plates are facilitating the acquirement of digital autoradiograms both due to an increased linear range and sensitivity. Reduced exposure time and a simplified development technique significantly lead to decreased time for data analysis allowing higher throughput.

Compared to autoradiography, useful pharmacological parameters such as affinity and density are also commonly characterized by the application of radioligands in tissue homogenate binding assays. This method has the advantage of producing results by measuring β-emitted radioactive decay with a liquid scintillation detector in an efficient manner[2]. Being performed in a multi-well approach, *e.g.,* in 96-well microtiter

plates, such assays are useful for screening of libraries of compounds and for a larger number of concentration-dependent relationships. On top of that, conducting saturation analysis with this setup is often more feasible compared to autoradiography, which displays a risk of oversaturated images with high radioligand concentrations. However, performing homologous displacement of a fixed low radioligand concentration with non-radioactive ligands in order to obtain K_d and B_{max} circumvents the problem of oversaturated images (**Figure 6**)[22]. Homogenate binding and autoradiography produce similar estimates for ligand affinity constants whereas tissue density of the protein of interest may be underestimated in homogenate binding. Thus, it has been proposed that cell membrane disruption concomitant with tissue homogenisation might result in receptor loss or altered binding conditions[3,33]. Moreover, errors in tissue dissection might produce homogenates contaminated with tissue from adjacent brain regions. In comparison, even complex binding patterns in small nuclei are visualized and differentiable due to the spatial anatomical resolution in autoradiography[3,33].

Immunohistochemistry also visualizes the distribution of a protein of interest anatomically. The method is capable of producing images with high anatomical resolution, as discrete tissue components can be identified at cellular level and even subcellular levels using electron microscopy. Expression levels are assessed based on the intensity of the staining. Nonetheless, absolute quantification of expression levels is difficult due to the lack of appropriate reference standards[39]. Moreover, immunohistochemistry is dependent on the availability of a selective, well-validated antibody which is often a problem in receptor research.

Before deciding on performing *in vitro* autoradiography, several considerations need to be made. First of all, post-mortem tissue preparation including sectioning as well as repeated freezing and thawing might influence the preservation of binding sites[2]. Furthermore, the method depends on the availability of an adequate radioligand, which displays high affinity and selectivity for the target in question[2]. The radioligand should not display significant binding to off-target sites, and it should also demonstrate a favourable kinetic profile. This is necessary because the ligand-target complex must stay intact during the scope of the experiment. Moreover, when suitable non-radioactive compounds exist, the introduction of the radionuclide might become a critical factor. Thus, the molecule of interest should be equipped with suitable functional groups for efficient radiolabelling, which enables production of radioligands with sufficiently high specific activity and chemical stability[40]. Another disadvantage of *in vitro* autoradiography is that the method only allows the use of an animal once. More elegantly is the extension to *in vivo* imaging methods such as position emission tomography (PET), which enables repeated scanning of the same animal and determination of occupancy and dynamic binding characteristics. PET is especially valuable for the study of higher mammals[41] and for dose optimization in pre-clinical studies [42,43,44].

Several modifications of the autoradiographic technique extend its application both in terms of the characterization of pharmacological targets in healthy and diseased states as well as in drug discovery and development. First of all, recent advances in imaging technology have led to the development of real-time autoradiography. Gas detectors of α/β-particles obviate the need for imaging plates or film by the direct measurement of disintegrations, thereby producing fast digital autoradiograms[45].

Moreover, *in vitro* autoradiography enables studies of the functionality of G protein-coupled receptors (GPCRs) on top of information about their anatomical distribution in post-mortem tissues. This variant of the method involves incubation of tissue sections with a radioactively labelled analogue of guanosine triphosphate (GTP), *i.e.,* [^{35}S]guanosine 5'-γ-thiotriphosphate ([^{35}S]GTPγS), together with a non-radioactive agonist of the GPCR. When the agonist binds and elicits a response of the GPCR, the incorporation of [^{35}S]GTPγS can be localized and quantified via autoradiography, which reflects only the activated receptor population[2,46,47].

Ex vivo autoradiography represents another version of the technique, which assesses the regional binding of a radioligand after administration to a live experimental animal. Following the sacrifice of the animal, cryosectioning of the tissue in question, and autoradiographic exposure result in autoradiograms which reflect the radioligand binding *in vivo*[2]. *Ex vivo* autoradiography is commonly employed within drug discovery and development programs in order to gain information on the pharmacokinetic profile of a lead compound, *i.e.,* its absorption, distribution, metabolism and excretion (ADME). Particularly whole-body autoradiography provides insight about drug distribution to all organs and tissues. However, determination of non-specific binding and quantification is more difficult compared to *in vitro* autoradiography due to possible metabolism and degradation of the radioligand and no means for washing away unbound ligand[48].

Autoradiography is also used for preliminary testing and characterization of PET ligands[4]. The high-energy radionuclides carbon-11 and fluorine-18 are most often used for PET ligands. PET is a prominent, non-invasive application for radioligands because quantifiable 3D images of the radioligand binding in a living animal can be obtained[11,40,49].

In vitro autoradiography using phosphor imaging plates represents a valuable assay method for the pharmacological characterization of ligand-target interactions. The method produces reproducible results by the employment of a relatively fast and simple protocol once optimal assay conditions have been established. Anatomical distribution of a protein of interest is determined within its native microenvironment, which allows the study of its physiological, pharmacological and pathological role in healthy and diseased post-mortem tissue of experimental animals as well as humans[2,47].

Disclosures

The authors declare no conflicts of interest.

Acknowledgements

The work was supported by the Lundbeck Foundation (Grant R133-A12270) and the Novo Nordisk Foundation (Grant NNF0C0028664). The authors thank Dr. Aleš Marek for the supply of [^{3}H]radioligand.

References

1. Upham, L. V., & Englert, D. F. in *Handbook of Radioactivity Analysis.* 1063-1127 Elsevier Inc. (2003).
2. Manuel, I. *et al.* Neurotransmitter receptor localization: From autoradiography to imaging mass spectrometry. *ACS Chemical Neuroscience.* **6**, 362-373 (2015).
3. Pavey, G. M., Copolov, D. L., & Dean, B. High-resolution phosphor imaging: validation for use with human brain tissue sections to determine the affinity and density of radioligand binding. *Journal of Neuroscience Methods.* **116**, 157-163 (2002).
4. Davenport, A. P. *Receptor Binding Techniques.* **897**, Humana Press (2012).
5. Busardò, F. P., Kyriakou, C., Napoletano, S., Marinelli, E., & Zaami, S. Clinical applications of sodium oxybate (GHB): from narcolepsy to alcohol withdrawal syndrome. *European Review for Medical and Pharmacological Sciences.* **19**, 4654-4663 (2015).
6. Wong, C. G. T., Gibson, K. M., & Snead, O. C. I. From the street to the brain: neurobiology of the recreational drug γ-hydroxybutyric acid. *Trends in Pharmacological Sciences.* **25**, 29-34 (2004).
7. Benavides, J. *et al.* High affinity binding site for γ-hydroxybutyric acid in rat brain. *Life Sciences.* **30**, 953-961 (1982).
8. Hechler, V., Gobaille, S., & Maitre, M. Selective distribution pattern of γ-hydroxybutyrate receptors in the rat forebrain and midbrain as revealed by quantitative autoradiography. *Brain Research.* **572**, 345-348 (1992).
9. Klein, A. B. *et al.* Autoradiographic imaging and quantification of the high-affinity GHB binding sites in rodent brain using ^{3}H-HOCPCA. *Neurochemistry International.* **100**, 138-145 (2016).
10. Gould, G. G., Mehta, A. K., Frazer, A., & Ticku, M. K. Quantitative autoradiographic analysis of the new radioligand [^{3}H](2*E*)-(5-hydroxy-5,7,8,9-tetrahydro-6*H*-benzo[α][7]annulen-6-ylidene) ethanoic acid ([^{3}H]NCS-382) at γ-hydroxybutyric acid (GHB) binding sites in rat brain. *Brain Research.* **979**, 51-6 (2003).
11. Jensen, C. H. *et al.* Radiosynthesis and evaluation of [^{11}C]3-hydroxycyclopent-1- enecarboxylic acid as potential PET ligand for the high-affinity γ-hydroxybutyric acid binding sites. *ACS Chemical Neuroscience.* 22-27 (2017).
12. Castelli, M. P., Mocci, I., Langlois, X., Gommeren, W., & Luyten, W. H. M. L. Quantitative autoradiographic distribution of γ-hydroxybutyric acid binding sites in human and monkey brain. *Molecular Brain Research.* **78**, 91-99 (2000).
13. Wellendorph, P. *et al.* Novel radioiodinated γ-hydroxybutyric acid analogues for radiolabeling and photolinking of high-affinity γ-hydroxybutyric acid binding sites. *Journal of Pharmacology and Experimental Therapeutics.* **335**, 458-464 (2010).
14. Vogensen, S. B. *et al.* New synthesis and tritium labeling of a selective ligand for studying high-affinity γ-hydroxybutyrate (GHB) binding sites. *Journal of Medicinal Chemistry.* **56**, 8201-8205 (2013).
15. Mehta, A. K., Muschaweck, N. M., Maeda, D. Y., Coop, A., & Ticku, M. K. Binding characteristics of the γ-hydroxybutyric acid receptor antagonist [^{3}H](2*E*)-(5-hydroxy-5,7,8,9-tetrahydro-6*H*-benzo[a][7]annulen-6-ylidene) ethanoic acid in the rat brain. *Journal of Pharmacology and Experimental Therapeutics.* **299**, 1148-53 (2001).
16. Kaupmann, K. *et al.* Specific γ-hydroxybutyrate-binding sites but loss of pharmacological effects of γ-hydroxybutyrate in $GABA_{B(1)}$-deficient mice. *Neuroscience.* **18**, 2722-2730 (2003).
17. Bay, T., Eghorn, L. F., Klein, A. B., & Wellendorph, P. GHB receptor targets in the CNS: Focus on high-affinity binding sites. *Biochemical Pharmacology.* **87**, 220-228 (2014).
18. Paxinos, G., & Franklin, K. B. J. *The mouse brain in stereotaxic coordinates.* Academic Press (2008).
19. Carletti, R., Tacconi, S., Mugnaini, M., & Gerrard, P. Receptor distribution studies. *Current Opinion in Pharmacology.* **35**, 94-100 (2017).
20. Wellendorph, P. *et al.* Novel cyclic γ-hydroxybutyrate (GHB) analogs with high affinity and stereoselectivity of binding to GHB sites in rat brain. *Journal of Pharmacology and Experimental Therapeutics.* **315**, 346-351 (2005).
21. Coenen, H. H. *et al.* Consensus nomenclature rules for radiopharmaceutical chemistry - Setting the record straight. *Nuclear Medicine and Biologly.* **55**, v-xi (2017).
22. DeBlasi, A., O'Reilly, K., & Motulsky, H. J. Calculating receptor number from binding experiments using same compound as radioligand and competitor. *Trends in Pharmacological Science.* **10**, 227-229 (1989).
23. Hulme, E. C. *Receptor-ligand interactions: a practical approach.* RL Press at Oxford University Press (1992).
24. Holm, P. *et al.* Plaque deposition dependent decrease in $5\text{-}HT_{2A}$ serotonin receptor in AβPPswe/ PS1dE9 amyloid overexpressing mice. *Journal of Alzheimer's Disease.* **20**, 1201-1213 (2010).
25. Thomsen, C., & Helboe, L. Regional pattern of binding and c-Fos induction by (R)- and (S)-citalopram in rat brain. *Neurochemistry.* **14**, 2411-2414 (2003).
26. López-Giménez, J. F., Mengod, G., Alacios, J. M., & Vilaró, M. T. Selective visualization of rat brain $5\text{-}HT_{2A}$ receptors by autoradiography with [^{3}H]MDL 100 ,907. *Naunyn-Schmiedeberg's Archives of Pharmacology.* **356**, 446-454 (1997).
27. Alexander, G. M., Schwartzman, R. J., Bell, R. D., Yu, J., & Renthal, A. Quantitative measurement of local cerebral metabolic rate for glucose utilizing tritiated 2-deoxyglucose. *Brain Research.* **223**, 59-67 (1981).
28. Kuhar, M. J., & Unnerstall, J. R. Quantitative receptor mapping by autoradiography: some current technical problems. *Trends in Neurosciences.* 49-53 (1985).
29. Kuhar, M. J., De Souza, E. B., & Unnerstall, J. R. Neurotransmitter receptor mapping by autoradiography and other methods. *Annual Review of Neuroscience.* 27-59 (1986).
30. Chen, H.-T., Clark, M., & Goldman, D. Quantitative Autoradiography of ^{3}H-Paroxetine Binding Sites in Rat Brain. *Journal of Pharmacological and Toxicological Methods.* **27**, 209-216 (1992).
31. Herkenham, M., & Pert, C. B. Light microscopic localization of brain opiate receptors: a general autoradiographic method which preserves tissue quality. *Journal of Neuroscience.* **2**, 1129-49 (1982).
32. Heimer, L., & Záborszky, L. *Neuroanatomical Tract-Tracing Methods 2 - Recent progress.* Plenum Press (1989).
33. Vessotskie, J. M., Kung, M. P., Chumpradit, S., & Kung, H. F. Quantitative autoradiographic studies of dopamine D_3receptors in rat cerebellum using [^{125}I]S(-)5-OH-PIPAT. *Brain Research.* **778**, 89-98 (1997).
34. Klein, A. B. *et al.* $5\text{-}HT_{2A}$ and $mGLU_2$receptor binding levels are related to differences in impulsive behavior in the roman low- (RLA) and high- (RHA) avoidance rat strains. *Neuroscience.* **263**, 36-45 (2014).
35. Johnston, R. F., Pickett, S. C., & Barker, D. L. Autoradiography using storage phosphor technology. *Electrophoresis.* **11**, 355-360 (1990).

36. Ito, T., Suzuki, T., Lim, D. K., Wellman, S. E., & Ho, I. K. A novel quantitative receptor autoradiography and in situ hybridization histochemistry technique using storage phosphor screen imaging. *Journal of Neuroscience Methods.* **59**, 265-271 (1995).
37. Amemiya, Y., & Miyahara, J. Imaging plate illuminates many fields. *Nature.* **336**, 89-90 (1988).
38. Kanekal, S., Sahai, A., Jones, R. E., & Brown, D. Storage-phosphor autoradiography: a rapid and highly sensitive method for spatial imaging and quantitation of radioisotopes*. *Journal of Pharmacological and Toxicological Methods.* 171-178 (1995).
39. Taylor, C. R., & Levenson, R. M. Quantification of immunohistochemistry - issues concerning methods , utility and semiquantitative assessment II. *Histopathology.* **49**, 411-424 (2011).
40. Uhl, P., Fricker, G., Haberkorn, U., & Mier, W. Radionuclides in drug development. *Drug Discovery Today.* **20**, 198-208 (2015).
41. Schmidt, K. C., & Smith, C. B. Resolution, sensitivity and precision with autoradiography and small animal positron emission tomography: Implications for functional brain imaging in animal research. *Nuclear Medicine and Biolology.* **32**, 719-725 (2005).
42. Piel, M., Vernaleken, I., & Rösch, F. Positron emission tomography in CNS drug discovery and drug monitoring. *Journal of Medicinal Chemistry.* **57**, 9232-9258 (2014).
43. Kristensen, J. L., & Herth, M. M. *In vivo* imaging in drug discovery. *Drug Design and Discovery.* (CRC Press, Taylor & Francis Grou), 119-135 (2017).
44. Cunha, L., Szigeti, K., Mathé, D., & Metello, L. F. The role of molecular imaging in modern drug development. *Drug Discovery Today.* **19**, 936-948 (2014).
45. Bailly, C. *et al.* Comparison of Immuno-PET of CD138 and PET imaging with $^{64}CuCl_2$and^{18}F-FDG in a preclinical syngeneic model of multiple myeloma. *Oncotarget.* **9**, 9061-9072 (2018).
46. Sóvágó, J., Makkai, B., Gulyás, B., & Hall, H. Autoradiographic mapping of dopamine-D_2/D_3receptor stimulated [^{35}S]GTPγS binding in the human brain. *European Journal of Neuroscience.* **22**, 65-71 (2005).
47. Sóvágó, J., Dupuis, D. S., Gulyás, B., & Hall, H. An overview on functional receptor autoradiography using [^{35}S]GTPγS. *Brain Research Reviews.* **38**, 149-164 (2001).
48. Solon, E. G. Use of radioactive compounds and autoradiography to determine drug tissue distribution. *Chemical Research in Toxicology.* **25**, 543-555 (2012).
49. Donnelly, D. J. Small molecule PET tracers in drug discovery. *Seminars in Nuclear Medicine.* **47**, 454-460 (2017).

